PROCEEDINGS OF SCIENCE

Recent theoretical ideas about dark sectors at the intensity frontier

Marco Costa[a,*]

[a] *Perimeter Institute for Theoretical Physics, 31 Caroline St N, Waterloo, ON N2L 2Y5, Canada*

E-mail: mcosta1@perimeterinstitute.ca

The nature of DM interactions is unknown. If the DM is not charged under SM forces, it can communicate with it through so-called portal interactions. Renormalizable portals have received lots of attention in the past. However, in some models non-renormalizable portals can appear naturally as the leading interaction with the SM. Inclusive production cross-sections through these portals can be computed in a model independent fashion. In this way it is possible to put general constraints on a large class of Dark Sectors. High intensity experiments such as beam dumps and neutrino experiments offer a great opportunity to test these models, through specific signatures such as displaced vertices.

Third Italian Workshop on the Physics at High Intensity (WIFAI2024)
12-15 November 2024
Bologna, Italy

*Speaker

https://pos.sissa.it/

PoS(WIFAI2024)033

1. Introduction

One of the open problems in particle physics is to understand the nature of Dark Matter (DM). Very few properties are known about the particles making up the DM (if at all). The two main ones are: i) the DM must interact weakly with the Standard Model (SM) particles, and ii) the DM must be stable on cosmological time scales. These two properties by themselves are too general to draw a clear picture of the Dark Sector (DS) nature.

An interesting open question is whether or not DM has extra interactions with the SM in addition to the gravitational force. A natural possibility is that DM is charged under SM forces. Given that this interaction must be weak, DM could be charged under the electroweak (EW) group. This scenario typically predicts DM to have a mass around the TeV scale, if the observed DM abundance is due to thermal freeze-out.

There are other models in which instead DM is predicted to be light, at the GeV scale or below. In this case, in order to avoid strong collider constraints, the DM must be neutral under the SM gauge group. Both these properties make it amenable to study such models at low energy, high intensity experiments. In this scenario the interaction between DM and SM is mediated by *portal operators*. These interactions are captured by lagrangian terms of the form $O_{\rm SM}O_{\rm DS}$, where both O are gauge-singlet local operators made by products of SM and DS fields respectively. At the renormalizable level, only three portals exists:

$$\epsilon F^{\mu\nu}F'_{\mu\nu}\ , \qquad yLHN\ , \qquad H^\dagger H(\lambda S^\dagger S + kS)\ , \tag{1}$$

where $F'_{\mu\nu}$ is the gauge field strength of a new singlet spin-1 field, the *dark photon* A'_μ, N is a heavy neutral lepton and S a scalar singlet. For a review of constraints on these portals we refer to Ref. [1]. However, there is no reason why such portals should appear first at the renormalizable level. We will consider interactions mediated by $D > 4$ dimensional portals of the form:

$$\frac{\kappa}{\Lambda_{\rm UV}^{D-4}}O_{\rm SM}O_{\rm DS}\ . \tag{2}$$

The $D = 5$ case has been thoroughly studied in the case where $O_{\rm DS}$ excites a single axion-like particle and $O_{\rm SM}$ is a SM topological density. However studies where such operator can excite multi-particle states (as for example in a current-current interaction) are not many (see for example [2, 3]). While at first this scenario might seem non-minimal, non-renormalizable portals appear each time the theory contains a heavy new particle charged under both the SM gauge group and (possibly) dark gauge group. To be as general as possible, we will consider also strongly coupled Dark Sectors. While the vast majority of portal models studied in the high-intensity experiments literature are weakly coupled, strongly coupled models are equally as motivated. An example of these are Hidden Valley models scenarios [4]. We will employ a formalism that can easily be adapted to describe both cases. We remark that we will not attempt to make any contact with cosmology, since the DM relic abundance might very well be set by internal DS dynamics, and hence be model-dependent.

2. Anatomy of non-renormalizable portals

For simplicity, in this section we will focus on DS bosonic operators $O_{\rm DS}$ with scaling dimension Δ_O. When describing the physics of these models, we will employ the language of strongly coupled

DS, but what we say holds also for a weakly coupled one. We assume that the DS is characterized by two scales: the UV cutoff of the portal $\Lambda_{\rm UV}$, which can be thought as the mass of a mediator between the DS and the SM, and the typical mass gap of the DS, $\Lambda_{\rm IR}$. To be more precise, we will define $\Lambda_{\rm IR}$ to be the mass of the *lightest DS particle* (LDSP), which we denote as ψ. At energies higher than $\Lambda_{\rm IR}$, it is useful to think of the DS states as *dark jet*, being composed by a multi-particle state of dark quarks and gluons. In this language, ψ would be a *dark hadron*.

In [5] it was realized that some inclusive observables, such as missing energy production (production of DS invisible states) at colliders and beam dumps, depend weakly on the details of the DS, and depend mostly on the quantum number of the DS operator $\mathcal{O}_{\rm DS}$. This is due to the fact that, by dimensional analysis, the differential DS production cross-section schematically scales as

$$\frac{\mathrm{d}\,\sigma_{\rm DS}}{\mathrm{d}\,p^2_{\rm DS}} \propto \kappa^2 \frac{\sqrt{p^2_{\rm DS}}^{\,2(D-4)-4}}{\Lambda_{\rm UV}^{2(D-4)}}\,, \tag{3}$$

where $p_{\rm DS}$ is the total 4-momentum of the produced DS states. For $D \geq 6$, the bulk of the cross-section comes from events with large $p_{\rm DS}$, far from the IR mass gap of the DS $\Lambda_{\rm IR}$. Hence the model-dependent resonance structure that appears near the threshold $\Lambda_{\rm IR}$ does not matter in the computation. By integrating (3) we get the following estimate for the total inclusive cross-section:

$$\sigma_{\rm DS} \propto \kappa^2 \frac{\sqrt{s}^{\,2(D-4)-2}}{\Lambda_{\rm UV}^{2(D-4)}}\,, \tag{4}$$

where $\sqrt{s}$ is the typical energy of the process. In other words, the Dark Sector enjoys approximate conformal invariance when considering production processes of energies $\sqrt{s}$ far from both the IR and UV scales.

The argument can be made more rigorous by exploiting the optical theorem, which relates the inclusive cross-section to the two point vacuum-vacuum correlator. Indeed inclusive DS production cross sections are obtained by integrating over the DS phase space, schematically indicated by $\mathrm{d}\,\Phi_{\rm DS}$, at fixed DS 4-momentum $p_{\rm DS}$:

$$\sigma_{\rm DS} \propto \int \frac{\mathrm{d}^4 p_{\rm DS}}{(2\pi)^4} \int \mathrm{d}\,\Phi_{\rm DS} |\langle {\rm DS}|\mathcal{O}_{\rm DS}|0\rangle|^2\,. \tag{5}$$

The optical theorem then allows us to rewrite:

$$\int \mathrm{d}\,\Phi_{\rm DS}|\langle {\rm DS}|\mathcal{O}_{\rm DS}(p_{\rm DS})|0\rangle|^2 = 2\,\mathrm{Im}\left[i\langle 0|T\left\{\mathcal{O}_{\rm DS}(p_{\rm DS})\mathcal{O}_{\rm DS}(-p_{\rm DS})\right\}|0\rangle\right] = c_{\mathcal{O}} A(\Delta_{\mathcal{O}}) p_{\rm DS}^{2(\Delta_{\mathcal{O}}-2)} \tag{6}$$

where T stands for time-ordering. In the last line we used approximate conformal invariance to fix the 2-point function. The *central charge* $c_{\mathcal{O}}$ is a free parameter related to the number of DS degrees of freedom excited by $\mathcal{O}_{\rm DS}$, while A is a known function of $\Delta_{\mathcal{O}}$.

3. Experimental signatures

In this section we want to understand how to test non-renormalizable portals. There are various signatures that can be studied, depending on the nature of the LDSP. By making contact with the strongly coupled regime language, we assume that on time-scales of order $1/\Lambda_{\rm IR}$ the DS jet confines into the LDSPs. This scale is typically much shorter than all the relevant detector scales, so it is safe to assume that this process happens promptly after production.

The number of LDSPs produced per jet, $n_{\rm LDSP}$, is a model dependent quantity. We model it after QCD in the strongly coupled case [6], while for the weakly coupled case we take an energy-independent value $n_{\rm LDSP} = 2$.

After production, the LDSPs can either escape the detector, decay inside it or even re-scatter against the detector's constituents. These processes will happen through a portal with the SM, possibly the same one responsible for DS production.

For example, the stability of the LDSP is governed by the following matrix element:

$$\langle 0|O_{\rm DS}|\psi\rangle \simeq f\Lambda_{\rm IR}^{\Delta_O - 2} \tag{7}$$

where $f \sim \sqrt{c_O}\Lambda_{\rm IR}/4\pi$ is a decay constant. Here we assumed that the LDSP is not protected by any symmetry which would otherwise set the matrix element to 0. This is typically expected in a strongly coupled scenario, where all the allowed portals are generated by the strong dynamics.

The second possibility is that the LDSPs scatter against the detector particles. If the scattering process is energetic enough, the ψ state can even disintegrate again into its DS constituents. The inclusive disintegration process depends on the following squared matrix element:

$$|\langle 0|O_{\rm DS}|\psi\rangle|^2 \,, \tag{8}$$

which is a model-dependent quantity. Even by making optimistic assumptions on the correlator in Eq 8, the signal is too small to be distinguished from neutrino background due to the smaller ψ flux reaching the detector. Hence LDSP disintegration doesn't typically lead to competitive bounds on $\Lambda_{\rm UV}$.

In the following subsections we are going to sketch the results for the signatures introduced, focusing on a strongly coupled DS interacting with the SM through the so-called *Z portal*:

$$\frac{k_Z}{\Lambda_{\rm UV}^2} H^\dagger i \overleftrightarrow{D}_\mu H\, J^\mu_{\rm DS} = \frac{k_Z}{\Lambda_{\rm UV}^2} v m_Z Z_\mu J^\mu_{\rm DS} \tag{9}$$

where $J^\mu_{\rm DS}$ is the conserved current associated to some DS symmetry. The last line follows by setting the Higgs to its vacuum expectation value $v/\sqrt{2}$. We will fix the values $k_Z, c_J = 1$.

3.1 Missing energy

If the LDSPs are stable (or long lived on detector timescales), then after being produced they escape the detector without interacting with it. The signature associated to this process is *missing energy* (ME). A protoypical example of this is mono-photon or mono-jet events with ME at colliders such as LEP or LHC respectively. Another class of ME signature is branching ratios of particles decaying into invisible states. The best of these latter constraints is the LEP measurement of the Z boson decay width, which can test whether the Z can decay invisibly into new DS states. This is shown in black in Fig. 2, together with mono-jet + ME searches at LHC (in gray) which give a slightly weaker bound. Bounds coming from decays of lighter mesons are weaker than the Z width given that the typical energy associated to such decays is much smaller than m_Z, and that DS production scales favorably with higher masses, as shown in Eq. (4).

3.2 Displaced vertices

In this section we consider LDSPs decaying on detector length scales. An estimate for the lifetime τ of the LDSP through the Z portal can be obtained through dimensional analysis:

$$\tau^{-1} \simeq \frac{k_J^2 f^2}{8\pi} \frac{\Lambda_{\rm IR}^3}{\Lambda_{\rm UV}^4} . \quad (10)$$

LDSPs decaying inside a detector lead to a displaced vertex (DV) signature: two (or more) SM particles appear without being preceded by any visibile track. Collider searches for DV signatures can test boosted lifetimes of order of tens of meters. Results for DV searches at colliders are shown in dashed gray in Fig. 2.

Longer lifetimes can instead be tested at beam dumps and beam-based neutrino experiments. The idea is to produce many LDSP particles by impinging a beam onto a fixed target. Residual SM particles are blocked by a shield, with the possible exception for neutrinos in some set-ups. Then the LDSPs and neutrinos will reach a detector positioned at $O(10^2)$ m away from the target. LDSPs decaying into such detectors give rise to DV signatures. There are essentially no SM backgrounds to DVs, since no SM particles reach the detector. Neutrino scatterings inside the detectors could be a source of background, but given the different topology of decays and scatterings events it is in principle possible to distinguish the two.

Here we consider experiments based on 120 and 400 GeV proton beam energies. For such energies there are three relevant production modes. First of all, the proton-nucleus interaction creates mesons, which may decay into lighter mesons and DS states, or completely annihilate into DS states. This requires $p_{\rm DS}^2 \leq \left(M_{\rm heavy} - M_{\rm light}\right)^2$ for the first scenario and $p_{\rm DS}^2 = M_{\rm heavy}^2$ for the second. We refer to these production channels as meson decay (MD) modes. For $p_{\rm DS}^2 \gtrsim \Lambda_{\rm QCD}^2$, the incoming proton is at high enough energies so one has to consider partonic processes involving constituents from the incoming proton and the nucleons in the target, and we refer to this as Drell-Yan (DY) production mode. For $p_{\rm DS}^2 \lesssim \Lambda_{\rm QCD}^2$, DS states can be produced from initial state emission, which we will refer to as Dark Bremsstrahlung (DB) mode. For each of these processes, the production cross section has a different differential distribution in $p_{\rm DS}^2$. Fig. 1 shows a comparison of the differential DS production cross-section for DY, DB and radiative MD mode, for Z portal, at 120 GeV beam energy. Features in the plots are due to scales present in form factors and PDFs which give a deviation from the naive scaling of Eq. 3. Overall, after integrating over the allowed $p_{\rm DS}^2$, we find that bremsstrahlung and DY production dominate for this portal over the contribution due to meson decays.

An estimate for the number of DV signal events can be obtained with the following formula:

$$S \simeq \frac{N_{\rm POT}}{\sigma_{pN}} \sigma_{\rm DS} \epsilon_{\rm geo} P_{\rm dec} \simeq \frac{N_{\rm POT}}{\sigma_{pN}} \sigma_{\rm DS} \epsilon_{\rm geo} n_{\rm LDSP} \left(e^{-l/(c\tau\gamma)} - e^{-(l+d)/(c\tau\gamma)} \right) \quad (11)$$

where $N_{\rm POT}$ is the total number of proton impinged on the target, σ_{pN} is the proton-target nucleus cross section evaluated at the typical energy of the beam, $\epsilon_{\rm geo}$ is the geometric acceptance of the detector, and $P_{\rm dec}$ is the probability for one of the LDSP particles to decay inside a detector of size $d \sim 10$ m positioned at a distance l after the target. γ is the average boost of a LDSP particle.

In Fig. 2 we show the results for past high intensity experiments (colored filled contours), and future projections (colored dashed contours) for 10 signal events. As can be seen, high intensity

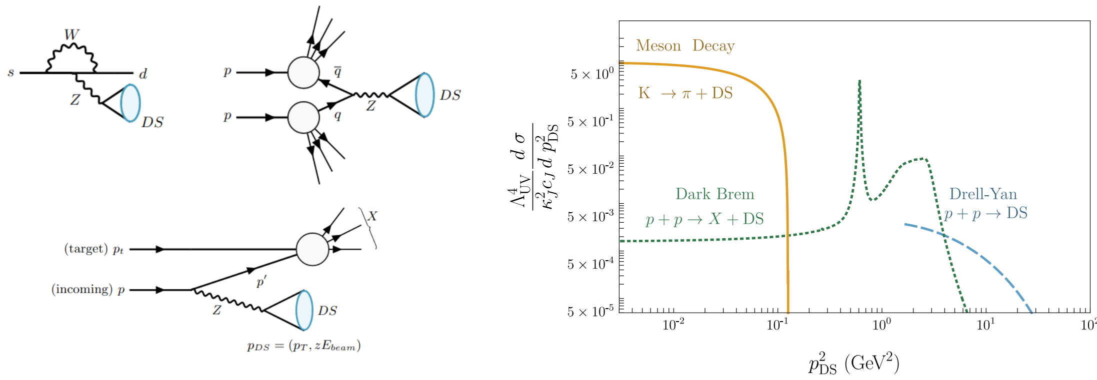

Figure 1: Left: Feynman diagrams for some of the relevant DS production modes. The cone represent a DS state (a *dark jet*). From top left, in clockwise order: radiative meson decay ($K \to \pi + \mathrm{DS}$), Drell-Yan, dark bremsstrahlung. **Right:** Relative importance of various production modes: the scaled differential cross-section for DS production at DUNE-MPD ($E_{\rm beam} = 120$ GeV) as a function of $p_{\rm DS}^2$ for various DS production modes (for Z portal). Solid yellow shows meson decay: $K \to \pi + \mathrm{DS}$ mode, dotted green line shows dark bremsstrahlung mode ($p + p \to X + \mathrm{DS}$), and dashed blue line shows Drell-Yan mode ($p + p \to \mathrm{DS}$). The reported cross-section is per proton-on-target, and is without the geometric acceptance factor $\epsilon_{\rm geom}$ (which at DUNE is estimated to be 10^{-3} for DY and meson modes and around 10^{-2} for DB mode).

experiments can provide the leading constraints for $\Lambda_{\rm UV}$ of order of a few TeVs and $\Lambda_{\rm IR}$ up to few GeVs, improving over collider bounds. For further details on the estimates we refer to [7].

3.3 Neutrino disintegration

While the disintegration of ψ has too little signal due to the small ψ flux reaching the detector, a similar signature arises with neutrinos when considering the fermionic non-renormalizable portal:

$$\frac{y}{\Lambda_{\rm UV}^{\Delta_N - 3/2}} LHO_N \tag{12}$$

where O_N is a composite right-handed neutrino operator. This can be thought as a model for describing neutrino partial compositeness. This interaction was considered in [8], where bounds coming from mesons and EW bosons decay into invisible were studied. The portal in Eq. 12 allows active neutrinos to scatter against electrons or nucleons inside the detector and disintegrate into their constituents. We dub this process *disintegration*. If the produced LDSPs are sufficiently long-lived, they escape detection, and the overall process mimicks neutrino neutral current (NC) interactions. If instead they decay back to the SM on detector length-scales, they can in principle give a visible signature. It can be shown that for $\Delta_N \geq 7/2$ the disintegration through a Z-initiated NC scattering is UV dominated (in the sense of Eq. 3). Hence we fix $\Delta_N = 7/2$. For this choice the LDSPs are long-lived, giving rise to the NC-like events. This anomalous contribution to NC processes could be studied at facilities with luminous, energetic neutrino beams ($E_\nu \sim 10 \div 10^2$ GeV), such as at DUNE (currently under construction), or at SHiP (approved) and Faser-ν (running) at CERN, while the strongest limits from past neutrino experiments come from NuTeV [9]. These neutrino fluxes are much larger than the LDSP flux, and the number of signal events $S_{\rm dis}$ can be large enough to be observable. The idea to separate the disintegration signal from the NC background $B_{\rm NC}$ is to exploit

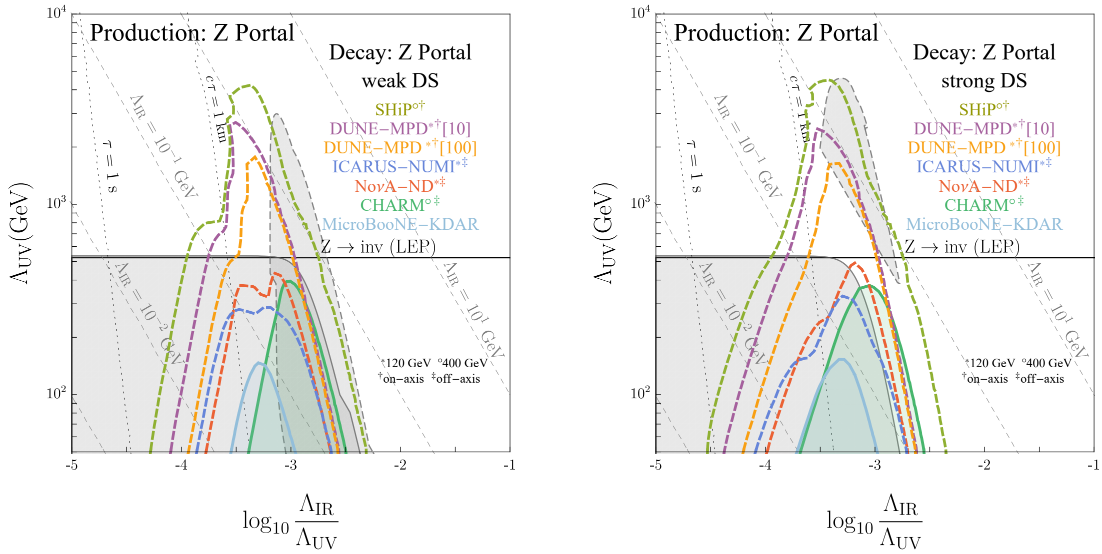

Figure 2: Constraints on DS production through the $D = 6$ Z portal and decay through the same Z portal at various high-intensity experiments. We have shown both the 10 event and the 100 event lines for DUNE. For comparison, bounds from high-energy colliders (obtained in ref. [5]) are also shown in gray (monojet searches with solid boundary and displaced vertex searches with dashed boundary). The left (right) plots assume weakly coupled (strongly coupled) dark dynamics. The exclusion from the Z invisible width measurement at LEP is shown by the horizontal solid black line. We restrict to $\Lambda_{\rm UV} > 50$ GeV for EFT validity. All plots assume $\kappa_J, c_J = 1$. Details on the computations and the experiments can be found in Ref. [7].

the different kinematics of the events: the latter has one massless particle in the final state, while the former has variable $p^2_{\rm DS}$. Loosely speaking, disintegration events are characterized by a less energetic, more forward SM final state given the higher energy flowing into the DS constituents with respect to the neutrino. The challenge of this signature is that it is not possible to fully reconstruct the kinematic of the event given that the the energy of the initial impinging neutrino is not exactly known. Scatterings against electrons are theoretically cleaner given the point-like nature of the electron. However they have lower $\sqrt{s}$ compared to scatterings against nucleons, given the lighter electron mass. As a consequence, the strongest bound comes from nucleon scatterings. We leave the details of the analysis to [9], and report the bounds in Fig. 3. Bounds coming from Higgs and Z invisible decays are at face value stronger, but they rely on the further assumption that the CFT description holds up to the electroweak scale. If this is not true, these bounds can potentially become weaker than the disintegration ones.

Acknowledgments

The author thanks the organizers for the opportunity to present this work. The author is supported in part by Perimeter Institute for Theoretical Physics. Research at Perimeter Institute is supported by the Government of Canada through the Department of Innovation, Science and Economic Development Canada and by the Province of Ontario through the Ministry of Research, Innovation and Science.

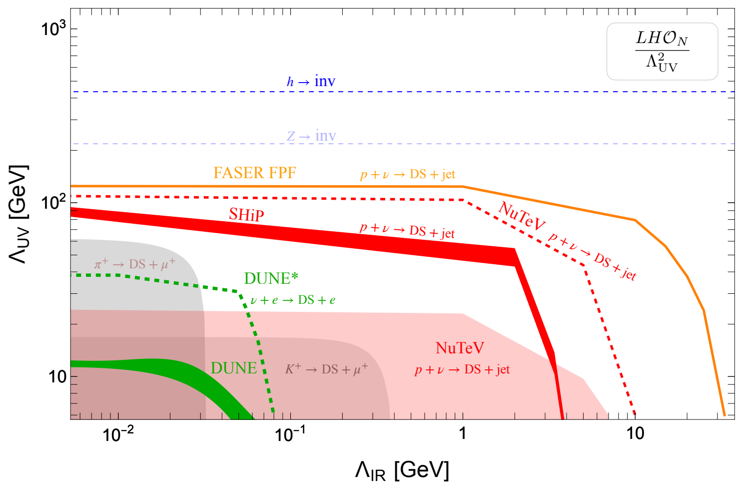

Figure 3: Plot of the portal in Eq. (12) for $\Delta_N = 7/2$, $c_N = 100$, $y = 1$. Only coupling to muon neutrino is assumed. **Red-shaded**: Excluded by NuTeV assuming $S_{DIS} = B_{NC}$. **Red dashed**: NuTeV projections assuming S_{DIS} to be less than the quoted uncertainty on NC measurements. **Red band**: SHiP sensitivity with different cuts on the final hadronic jet. **Orange**: Forward Physics Facility sensitivity. **Green band**: DUNE sensitivity; stronger with tau-optimized flux, **dashed** for narrower ν flux $\delta E_\nu / E_\nu = 20\%$. **Dark Blue**: Higgs invisible branching ratio constraints. **Light Blue**: Z invisible branching ratio constraints. **Gray-shaded**: Excluded by meson decays. Details on the experiments can be found in Ref. [9].

References

[1] B. Batell, N. Blinov, C. Hearty and R. McGehee, *Exploring Dark Sector Portals with High Intensity Experiments*, in *Snowmass 2021*, 7, 2022 [2207.06905].

[2] E. Bertuzzo and M. Taoso, *Probing light dark scalars with future experiments*, *JHEP* **03** (2021) 272 [2011.04735].

[3] L. Darmé, S.A.R. Ellis and T. You, *Light Dark Sectors through the Fermion Portal*, *JHEP* **07** (2020) 053 [2001.01490].

[4] M.J. Strassler and K.M. Zurek, *Echoes of a hidden valley at hadron colliders*, *Phys. Lett. B* **651** (2007) 374 [hep-ph/0604261].

[5] R. Contino, K. Max and R.K. Mishra, *Searching for elusive dark sectors with terrestrial and celestial observations*, *JHEP* **06** (2021) 127 [2012.08537].

[6] R.K. Ellis, W.J. Stirling and B.R. Webber, *QCD and collider physics*, vol. 8, Cambridge University Press (2, 2011), 10.1017/CBO9780511628788.

[7] M. Costa, R.K. Mishra and S. Verma, *Model agnostic probes of dark sectors at neutrino experiments*, *Phys. Rev. D* **108** (2023) 035041 [2211.13253].

[8] Z. Chacko, P.J. Fox, R. Harnik and Z. Liu, *Neutrino Masses from Low Scale Partial Compositeness*, *JHEP* **03** (2021) 112 [2012.01443].

[9] M. Borrello, M. Costa and D. Redigolo, *Invisible jets from composite neutrinos*, 2507.12527.